

# Scintillation light produced by low-energy beams of highly-charged ions

M. Vogel<sup>a,\*</sup>, D.F.A. Winters<sup>a</sup>, H. Ernst<sup>b</sup>, H. Zimmermann<sup>c</sup>, and O. Kester<sup>a</sup>

<sup>a</sup>*GSI, Planckstrasse 1, D-64291 Darmstadt, Germany*

<sup>b</sup>*Johannes-Gutenberg-Universität Mainz, Staudingerweg 7, D-55099 Mainz, Germany*

<sup>c</sup>*Ludwig-Maximilians-Universität, Schellingstrasse 4, D-80799 München, Germany*

---

## Abstract

Measurements have been performed of scintillation light intensities emitted from various inorganic scintillators irradiated with low-energy beams of highly-charged ions from an electron beam ion source (EBIS) and an electron cyclotron resonance ion source (ECRIS). Beams of xenon ions  $\text{Xe}^{q+}$  with various charge states between  $q=2$  and  $q=18$  have been used at energies between 5 keV and 17.5 keV per charge generated by the ECRIS. The intensity of the beam was typically varied between 1 and 100 nA. Beams of highly charged residual gas ions have been produced by the EBIS at 4.5 keV per charge and with low intensities down to 100 pA. The scintillator materials used are flat screens of P46 YAG and P43 phosphor. In all cases, scintillation light emitted from the screen surface was detected by a CCD camera. The scintillation light intensity has been found to depend linearly on the kinetic ion energy per time deposited into the scintillator, while up to  $q=18$  no significant contribution from the ions' potential energy was found. We discuss the results on the background of a possible use as beam diagnostics e.g. for the new HITRAP facility at GSI, Germany.

*Key words:* highly-charged ions, ion-surface interaction, scintillation light, beam diagnostics

*PACS:* 34.50.Dy, 79.20.Rf, 78.55.-m, 41.75.Ak

---

## 1. Introduction

Beams of heavy highly-charged ions are typically produced at energies in the high keV/u to MeV/u range. Correspondingly, the energy deposition of such a beam into a solid target, e.g. a scintillation screen, is high and the subsequent light emission intense. At the HITRAP facility [1,2], beams of highly-charged ions will be produced by stripping, using the GSI accelerator facility. Stripping of heavy ions to high charge states requires beam energies of several hundred MeV per nucleon. At HITRAP these ions will subsequently be decelerated to ener-

gies of only a few keV per charge. Beam intensities at HITRAP will be below a  $\mu\text{A}$  during a bunch of  $\mu\text{s}$  duration. It will be necessary to have beam diagnostic instrumentation at hand which is able to detect such low-energy particle beams. Especially, the low kinetic energy deposition into the scintillator and its possible charging up, leading to a subsequent deflection of the low-energy beam, may be obstacles for optical detection of charged particle beams.

Numerous scintillation experiments have been performed with a wide variety of scintillator materials, however mostly photon or electron beams have been used to stimulate scintillation [3]. Ion beam experiments have been predominantly performed with intense beams of MeV/u kinetic energies, see for example [4,5,6]. For low-energy beams both exper-

---

\* Corresponding author.

*Email address:* m.vogel@gsi.de (M. Vogel).

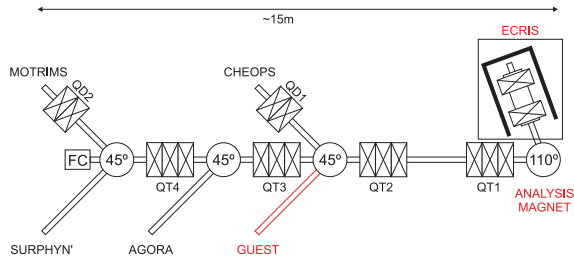


Fig. 1. ECR ion source setup at KVI, Groningen with its "guest" port, where the present experiments have been performed.

imental [7] and theoretical [8] results are available, however no high charge states have been considered. Information on scintillation light produced by low-intensity, highly-charged ion beams in the energy region of few keV per charge is sparse and therefore requires a more detailed study. Generally, it is known that for ions the scintillation light yield is roughly 50 to 70% of that for electrons and about 25 to 50% of that for photons [3]. Scintillator materials like the presently used P43 phosphor screen emit on average 36 photons per keV deposited kinetic energy, P46 (YAG) emits about half of that [3].

In the following, we present the results of an experimental study of scintillation light produced by low-energy highly-charged ion beams impinging on P43 and P46 scintillator screens.

## 2. Experimental setup and procedure

The measurements have been performed using an Electron Cyclotron Resonance Ion Source (ECRIS) [9,10] setup at the KVI, Groningen and the MAXE-BIS setup at GSI, which is described in detail in [11]. Details of the KVI-ECRIS have been given in [12]. In case of the ECRIS, highly-charged ions are continuously produced and transferred to the analysis magnet which is a mass-over-charge ( $m/q$ ) filter. The ion species of interest is selected by an appropriate choice of the field strength in the analysis magnet. The beam energy is defined by the potential applied to the source. Values up to 20 keV can be chosen with an uncertainty of about 50 V. Ion optical elements then guide the beam to the "guest" port shown in figure 1.

The MAXEBIS delivers a pulsed beam and therefore the CCD-camera was triggered by the signal of the extraction pulser. Depending on the confinement time of the ions in the EBIS, the repetition rate is typically of the order of 10 to 100 Hz. The ion

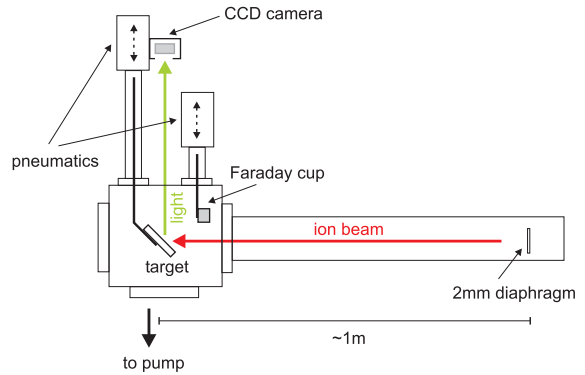


Fig. 2. Scheme of the experimental setup. For details see text.

pulse length corresponds to 30 - 50  $\mu$ s, typical beam energies are of the order of a few keV per charge.

The scintillator screens are irradiated by the ion beam under an angle of  $45^\circ$  and a CCD camera (model Basler A311f) monitors the scintillation light emitted from the screen perpendicular to the beam axis, see figure 2. A Faraday cup (30 mm diameter) with secondary electron suppression can be moved into the beamline for a measurement of the beam current. The uncertainty of this measurement is estimated to be about 1 %. However, temporal fluctuations of the beam intensity can amount up to 10 % of the measured value.

The P43 target is an aluminium disk of 70 mm diameter coated with about 40-50  $\mu$ m of amorphous  $\text{Gd}_2\text{O}_2\text{S:Tb}$ . It emits light between 360 nm and 680 nm with a spectral peak wavelength of 545 nm (green) and has an average decay time (90% to 10% intensity) of 1.0 ms. The P46 YAG is a  $\text{Y}_3\text{Al}_5\text{O}_{12}\text{:Ce}$  crystal which also emits green light with a spectral peak wavelength of 550 nm and has an average decay time of 70 ns. Additionally, we have used a P46 YAG screen identical to the first one, but coated with  $1 \mu\text{g}/\text{cm}^2$  of aluminium to build a conducting surface and possibly prevent it from charging up by the ion beam.

In all cases it may be assumed that the ions deposit their complete kinetic energy into the target, i.e. that the scintillation signal represents the beam characteristics well. This is corroborated by application of the Bethe-Bloch equation for the energy loss of the ion in the target material [3], presently leading to loss coefficients of the order of GeV/mm and correspondingly to extremely low penetration depths which are well below the scintillator thickness. Also, the present scintillators are highly transparent at their emission wavelengths such that nearly all pro-

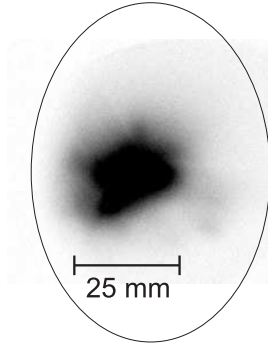


Fig. 3. Beam spot on the P46 scintillator screen for 30 nA of  $\text{Xe}^{7+}$  at 10 keV/q. For the sake of demonstration, the picture has been color inverted and shows the screen border.

duced light is emitted. At the low beam intensities presently used, saturation effects of the scintillators are not expected. The experiments have been performed at room temperature ( $T \approx 300$  K) and at a residual gas pressure of a few  $10^{-7}$  mbar. Due to the low ion beam currents and energies used, heating of the target is not expected. The temporal stability of the scintillation light signal can be estimated from the measured fluctuations to be well within 10% of the observed intensity within a time interval of about 15 minutes.

### 3. Results

Figure 3 shows a typical picture of the beam spot on the scintillator as seen by the CCD camera. For the sake of demonstration, this picture has been taken at the highest camera sensitivity and is colour inverted. The ellipse represents the scintillator surface as seen by the camera under the  $45^\circ$  angle (see figure 2). In the further evaluation, the amount of scintillation light ("intensity") is determined from unsaturated greyscale pictures ( $646 \times 494$  pixels) as the sum of all greyscale values. The amount of background light has been measured and subtracted from all images before further analysis.

The scintillation light intensity is found to depend linearly on the ion beam current (see figure 4). This is in agreement with both theoretical considerations and previous experimental results on singly and multiply charged ions at high energies [4,5,6,13,14,15]. For fixed beam parameters the kinetic energy deposited into the scintillator is proportional to the beam current. As an example, figure 4 shows the intensity from the P46 target as a function of the ion beam current for  $\text{Xe}^{3+}$ ,  $\text{Xe}^{5+}$  and  $\text{Xe}^{7+}$  ions at an energy of 10 keV/q. The dependence is linear as

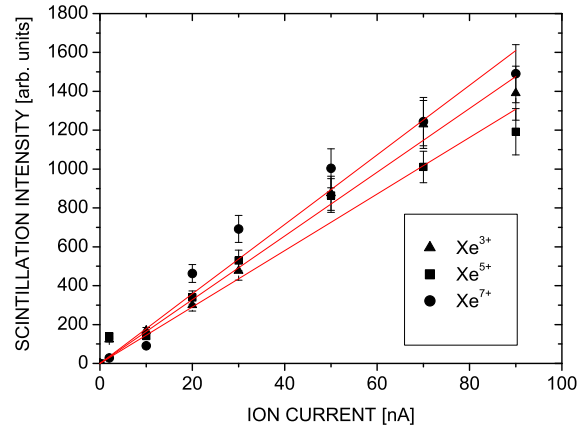


Fig. 4. Detected scintillation light from the P46 target as a function of the ion beam current for  $\text{Xe}^{3+,5+,7+}$  at an energy of 10 keV/q. The line is a weighted linear fit to the data.

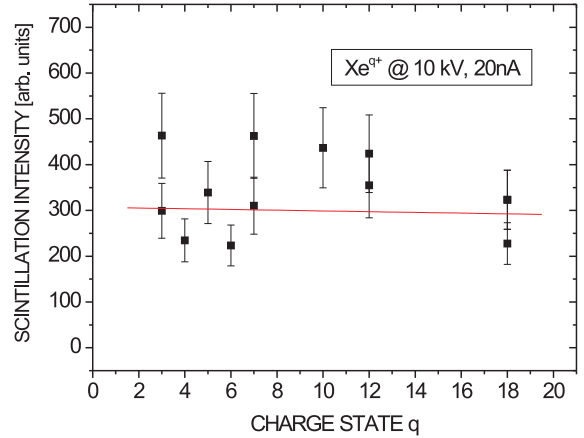


Fig. 5. Scintillation light intensity from the P46 screen as a function of the ion charge state  $q$  measured with 20 nA beams of  $\text{Xe}^{q+}$  ions at 10 keV/q. The line is a weighted linear fit to the data.

suggested by the fits. This linear relationship holds true for all ion species under observation and for all kinetic energies used in the present investigation.

From figure 4 it can also be concluded that there is no significant effect of the charge state on the intensity. To quantify this further, the charge-state dependence has been investigated in more detail. Figure 5 shows the relation between charge state and intensity for 20 nA beams of  $\text{Xe}^{q+}$  ions at an energy of 10 keV per charge on the P46 target.

The scatter of this data exceeds the 10% statistical uncertainty given by beam intensity fluctuations (see above). This is attributed to surface-related effects, such as surface contamination (residual gas) and ion beam sputtering of the surface (cleaning). However, within the scatter of the data, there seems

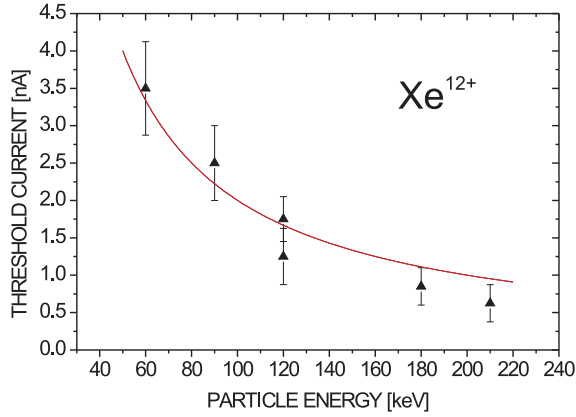


Fig. 6. Ion beam current threshold as a function of particle energy for a given particle, here  $\text{Xe}^{12+}$ . The line is a  $1/E$  fit to the data.

to be no obvious dependence on the charge state. Since the ion beam current  $I$  is kept constant, an increase in charge state  $q$  leads to a corresponding decrease of the ion number current proportional to  $1/q$ . At the same time, since the acceleration voltage is fixed, the kinetic energy per particle increases proportional to  $q$ , such that the total amount of deposited energy per time is unchanged.

An important number for practical use of scintillators as beam diagnostics is the "threshold current". This is the minimum current required to produce an optically detectable scintillation signal.

Figure 6 shows the dependence of the threshold current on the particle energy for  $\text{Xe}^{12+}$ . The threshold current shows a  $1/E$  dependence, where  $E$  is the kinetic energy of the particle. This can be understood as follows: With more kinetic energy per particle, less particles are needed to produce the same intensity. For fixed  $q$ , this means that the threshold current decreases.

All ECRIS threshold data was taken at the highest CCD camera sensitivity. This implies that  $3.65 \times 10^7$  photons per observation time of 80 ms are required for a non-vanishing signal.

With the MAXEBIS, the dc-threshold current has been measured to be 100 pA for a focused  $\text{C}^{4+}$ -beam at a kinetic energy of 4.5 keV/q. However, due to the focused beam (spotsizes of only a few mm), the apparent threshold current is lower than for the ECRIS measurements by the ratio of the spot areas. This is also a practical means to lower the threshold current, as long as the spotsize can be controlled well and the focusing does not lead to saturation of the scintillation material.

The information on the threshold current can, to-

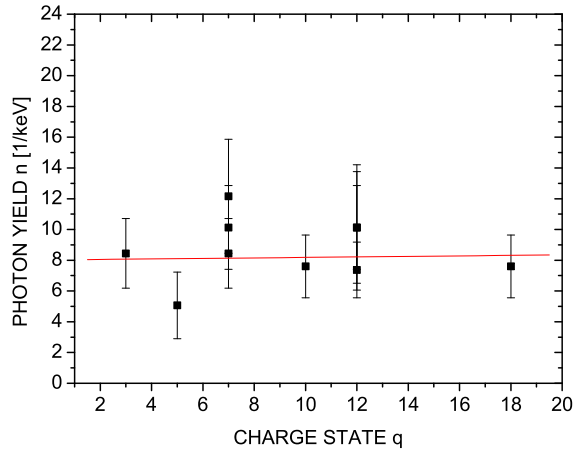


Fig. 7. Photon yield  $n$  in units of  $1/\text{keV}$  as a function of the charge state  $q$  of the xenon ions. The line is a linear fit to the data.

gether with the known camera sensitivity and beam parameters, be used to extract information on the photon yield  $n$  of the scintillator. At the threshold current  $I$ , the particle current is  $I_n = I/qe$ , where  $e$  is the elementary charge and  $q$  is the charge state of the ion. The kinetic energy deposited per second into the scintillator is  $E_{kin} = qI_n U$ , where  $U$  is the ion acceleration voltage. We assume that at this value, the light emission is just at the camera threshold, i.e.  $3.65 \times 10^7$  photons are detected within 80 ms.

We define the photon yield of the scintillator as

$$n = \frac{\text{number of emitted photons}}{\text{kinetic energy deposition}}. \quad (1)$$

Expressing this in terms of the experimental variables yields

$$n = \frac{N}{ABE_{kin}} = \frac{Ne}{ABIU}. \quad (2)$$

Here  $A = 5 \times 10^{-4}$  is a solid angle correction for the fraction of emitted photons seen by the camera, given by  $A = r^2/(4d^2)$  where  $r = 0.02$  m is the camera lens aperture radius and  $d = 0.45$  m is the screen-lens distance.  $N = 3.65 \times 10^7$  is the threshold photon number and  $B = 0.08$  is the fraction of a second during which photons are detected.

Figure 7 shows the photon yield  $n$  in units of  $1/\text{keV}$  as a function of the charge state  $q$ . The line is a linear fit to the data and its slope is in agreement with zero. Thus, the photon yield is found not to depend on the ions' charge state, but to have a constant mean value of  $n = 8.1 \pm 1.8$ .

This is in agreement with the independence of equation (2) on  $q$  and with the above statement that

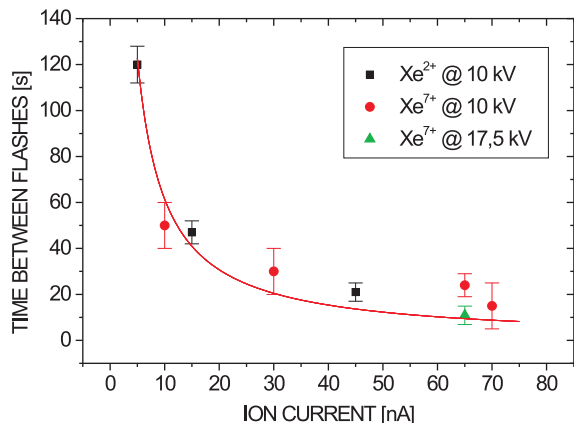


Fig. 8. Average time between observed flashes at the P43 target as a function of ion beam current  $I$ . The line is a  $1/I$  fit to the data (see text).

for ions the photon yield of P46 is between 25% and 50% of 18 photons per keV of deposited energy. Furthermore, it corroborates the above discussed independence of the scintillation signal on the ions' charge state (see figure 5).

Under certain conditions, the P43 target showed charging phenomena expressed by a continuous increase in emitted scintillation light from zero to a maximum value and an intense subsequent flash. This has been observed exclusively for multiply-charged particles of energies of and above 10 keV per charge. The light intensity during the flash is about two orders of magnitude higher than the brightest regular intensity before the flash. The duration of the flash is well below a single frame of the CCD camera, which is about 80 ms. As long as the beam hits the target, this phenomenon is repeated at a constant flashing rate depending on the ion beam parameters.

Figure 8 shows the average time between observed flashes of the P43 target as a function of the ion beam current for different multiply-charged ions at different ion energies. The necessary charging time between flashes shows a  $1/I$  dependence, as can be seen from the fit in figure 8. In contrast, the P46 YAG screens have not shown any of these phenomena under the same conditions. The flashing phenomenon might, however, be used for a measurement of the ion beam current in situations where light detection is difficult and it is only possible to observe the very bright flashes. In this kind of situation, the flashing rate could be used as a measure of the ion beam current.

Apparently, the thin amorphous layer of P43 on

eloxed aluminium has a substantially higher electrical resistance than the P46 crystal, for which no charging phenomenon was observed for beam currents up to one  $\mu\text{A}$ . In contrast to the observations made in [16], no temporal decay of the scintillation efficiency could be observed for both P43 and P46, which appear to keep constant efficiencies over beam times of hours. However, P43 showed similar surface anomalies as those described in [16], i.e. a local change in colour from white to brown, but without any macroscopically observable change in structure or in scintillation efficiency. This change in colour may be attributed to the flashing phenomenon, which presumably is connected with high currents which may give rise to changes in the surface composition. In situations with high-intensity high-energy beams, it was found that carbon from cracked residual gas molecules had been adsorbed to the target surface thus changing its composition and colour [17]. Although the presently used beam intensities and energies are several orders of magnitude away from those conditions, it may still be assumed that the very intense flashes across the screen surface are connected with temperatures high enough to crack residual gas molecules which then are adsorbed onto the surface.

The metal-coated P46 screen was found to show no observable scintillation light for any of the beam parameters used. Thus, a number of high-current measurements in the  $\mu\text{A}$  region were performed using beams of  $\text{He}^+$  and  $\text{O}^{2+}$ . However, up to beam currents of 1  $\mu\text{A}$ , no scintillation was detected. The metal coating is believed to be thin enough (about 10 monolayers) for the ions to penetrate even at low energies. Yet, scintillation was hindered by the metal coating for unknown reasons. This behaviour is unexpected and requires a more detailed study.

#### 4. Summary and conclusion

We have performed scintillation light measurements with continuous and pulsed beams of low-energy, highly-charged ions on P43 and P46 scintillator screens. While the metal coated P46 screen did not show any observable scintillation signal for any beam current up to 1  $\mu\text{A}$ , both uncoated P43 and P46 screens showed signals for beam currents above roughly 1 nA for continuous beam from the ECRIS and about 100 pA for focused and pulsed beams from the MAXEBIS. The intensity of this signal has been found to increase linearly with the beam current, in agreement with previous findings

at high energies and theoretical considerations. This behaviour is found to be independent of the charge state of the ions, at least up to  $\text{Xe}^{18+}$ . The amount of produced scintillation light thus seems to depend only on the amount of kinetic energy deposited into the scintillator and not on the charge state of the ions. This holds true both for the observed intensity and the photon yield per deposited energy. The P43 screen shows wear and charging phenomena which may obstruct its use under certain conditions, i.e. for high particle energies or intense beams. The uncoated P46 seems to be best suited for diagnostics of low-energy beams of highly-charged ions, e.g. at HITRAP. This is especially due to the fact that P46 produces sufficient intensity while not showing any signs of charging up even when highly charged ions are used. It is yet unclear if the present results apply also to ions with much higher charge states, since secondary effects due to the high potential energy cannot be ruled out. Also, potential sputtering [18,19] could become significant for very highly charged ions. This needs experimental clarification when such ion beams become available. The fast scintillation decay of P46 may evoke the need for a more sensitive camera system than presently used when a pulsed beam is considered. This requirement, however, can easily be met.

## 5. Acknowledgements

We are grateful for the fruitful collaboration with T. Schlathölter and R. Hoekstra from KVI, Groningen, Netherlands. We also thank T. Hoffmann and P. Forck (GSI) for helpful discussions.

## References

- [1] T. Beier *et al.*, Nucl. Instr. Meth. B **235** (2005) 473.
- [2] H.-J. Kluge *et al.*, Proceedings of the Memorial Symposium for Gerhard Soff, Topics in Heavy Ion Physics (Eds. Walter Greiner and Joachim Reinhardt) (2005).
- [3] W.R. Leo, *Techniques for Nuclear and Particle Physics Experiments*, Springer, Berlin, Heidelberg (1994).
- [4] P. Heeg, *Intensity measurements of heavy ion beam from SIS*, Proceedings of the EPAC conference (1992) 1100.
- [5] P. Heeg and O. Keller, *A scintillator photodiode beam intensity monitor*, Proceedings of the EPAC conference (1994) 1725.
- [6] M. Re *et al.*, *Production of thin scintillating films for ion beam monitoring devices*, Proceedings of the Particle Accelerator Conference (2005) 808.
- [7] L. Cosentino and P. Finocchiaro, Nucl. Instr. Meth. B **211** (2003) 443.
- [8] H.S. Cruz-Galindo *et al.*, Nucl. Instr. Meth. B **194** (2002) 319.
- [9] Geller, R., *Electron Cyclotron Resonance Ion Sources and ECR plasmas*, IOP Publishing Ltd., London 1996.
- [10] F. Bourg, R. Geller and B. Jacquot, Nucl. Instr. Meth. A **254** (1987) 13.
- [11] O. Kester, H. Zimmermann, R. Becker and M. Kleinod, Rev. Sci. Instr. **77** (2006) 03B102.
- [12] A.G. Drentje, H.R. Kremers, J. Mulder and J. Sijbring, Rev. Sci. Instr. **69** (1998) 728.
- [13] P. Antonini *et al.*, Nucl. Instr. Meth. A **488** (2002) 591.
- [14] G. Blasse and B.C. Grabmaier, *Luminescent Materials*, Springer, Berlin, Heidelberg (1994).
- [15] G.F. Knoll, *Radiation Detection and Measurement*, Wiley and Sons, New York (1998).
- [16] T. Sieber *et al.*, Proc. of the EPAC06 conference, Edinburgh, UK, 2006.
- [17] T. Hoffmann (GSI), private communication (2006).
- [18] G. Hayderer *et al.*, Phys. Rev. Lett. **86** (2001) 3530.
- [19] S.T. de Zwart *et al.*, Surf. Sci. **177** (1986) L939.